International Forum on Aeroelasticity and Structural Dynamics
IFASD 2019
9-13 June 2019, Savannah, Georgia, USA

WHIRL FLUTTER-RELATED CERTIFICATION ACCORDING TO FAR/CS 23 AND 25 REGULATION STANDARDS

Jiří Čečrdle[1]

[1] Czech Aerospace Research Centre (VZLU)
Prague, 199 05, Czech Republic
cecrdle@vzlu.cz

Keywords: IFASD, aeroelasticity, stick model, full-span model.

Abstract: Submitted paper describes the methodologies of compliance with whirl flutter-related requirements of FAR / CS 23 and 25 regulation standards. Methodologies are demonstrated on the example of a twin wing-mounted engine aircraft. For the compliance with FAR / CS 23 standard, two approaches are used: 1) standard approach to comply with the main requirement (§629(e)(1)) and 2) optimisation-based approach to comply with the requirement of parameter variations (§629(e)(2)). Standard approach, in which analyses are performed sequentially (state-by-state), is good for the nominal state. Optimisation-based analysis is used to calculate stability margins, which are then used for evaluation of stability reserve in terms of specific parameters. For compliance with FAR / CS 25 standard, the additional requirements to analyse specific failure states and adverse condition states are described.

1 INTRODUCTION

Whirl flutter is a specific type of aeroelastic flutter instability that may appear on turboprop aircraft. The instability is driven by motion-induced unsteady aerodynamic propeller forces and moments acting on the propeller plane. Rotating parts, such as a gas turbine engine rotor or a propeller increase the number of degrees of freedom and generate additional dynamic and aerodynamic forces and moments. In addition, there is also an aerodynamic interference effect between a rotating propeller and the structure of a nacelle and a wing. Whirl flutter may cause unstable vibration of a propeller mounting, leading to the failure of an engine installation or an entire wing. It has been a cause of several serious accidents.

Therefore, airworthiness regulation standards include also requirements related to the whirl flutter. These requirements are, however, specified just generally without any detailed description of the acceptable means and methodologies of compliance. Thus, the methodology of compliance must be negotiated in advance and approved either by the certification authority or by a compliance verification engineer.

Submitted paper describes the methodologies of compliance with whirl flutter-related requirements of FAR / CS 23 regulation standard (commuter and utility aircraft) and of FAR / CS 25 regulation standard (larger transport aircraft). Methodologies are demonstrated on the example of a twin wing-mounted engine aircraft.

2 THEORETICAL BACKGROUND

The principle of the whirl flutter phenomenon is outlined on a simple mechanical system with two degrees of freedom. The propeller and hub are considered as rigid. A flexible engine mounting is represented by two rotational springs of stiffnesses K_Ψ and K_Θ, as illustrated in figure 1.

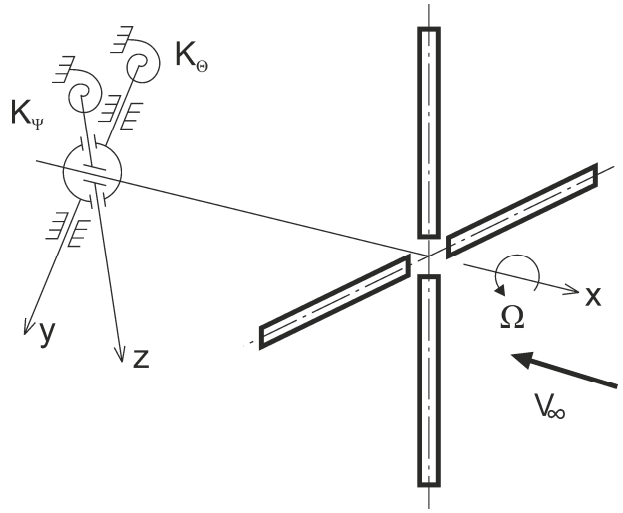

Figure 1: Gyroscopic system with propeller

Such a system has two independent mode shapes (yaw and pitch) with angular frequencies ω_Ψ and ω_Θ. For a propeller rotation with angular velocity Ω, the primary motion changes and the gyroscopic effect causes both independent mode shapes to merge into a whirl motion. The axis of rotation of the propeller exhibits an elliptical movement. The trajectory of this elliptical movement depends on both angular frequencies ω_Ψ and ω_Θ. The orientation of the gyroscopic movement is backward relative to the propeller rotation for the mode with the lower frequency (backward whirl mode) and forward relative to the propeller rotation for the mode with the higher frequency (forward whirl mode). Because the yaw and pitch motions have a 90° phase shift, the mode shapes in the presence of gyroscopic effects are complex.

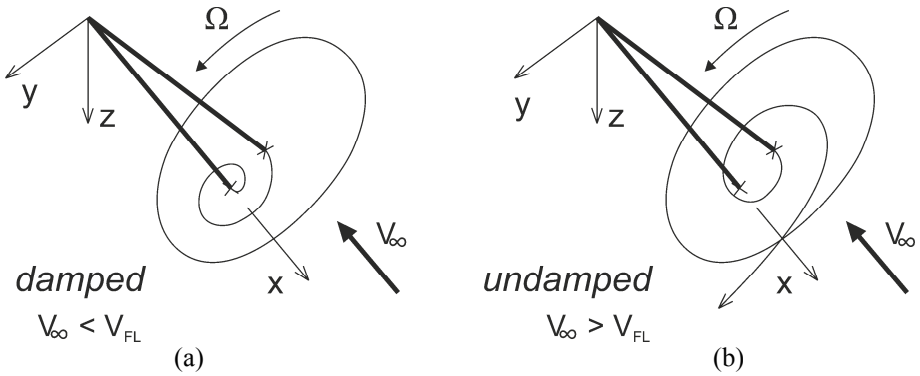

Figure 2: Stable (a) and unstable (b) states of gyroscopic vibrations for the backward flutter mode

The gyroscopic motion results in changes in the propeller blades' angles of attack, consequently leading to unsteady aerodynamic forces. These forces may, under specific conditions, induce whirl flutter instability. The flutter state is defined as the neutrally stable state with no damping of the system, and the corresponding airflow ($V_\infty = V_{FL}$) is called the critical flutter speed. If the air velocity is lower than flutter speed ($V_\infty < V_{FL}$), the system is stable and the gyroscopic motion is damped (figure 2a). If the airspeed exceeds the flutter

speed ($V_\infty > V_{FL}$), the system becomes unstable, and the gyroscopic motion is divergent (figure 2b).

An analytical solution is sought to determine the aerodynamic force caused by the gyroscopic motion on each of the propeller blades. The equations of motion were derived for the system shown in figure 1. The kinematical scheme is shown in figure 3. We select three angles (φ, Θ, Ψ) as the independent generalised coordinates. The rotating part is assumed to be cyclically symmetric with respect to both mass and aerodynamics (i.e., a propeller with a minimum of three blades). The propeller angular velocity is considered constant ($\varphi = \Omega\, t$). Non-uniform mass moments of inertia of the engine with respect to the pitch and yaw axes ($J_Z \neq J_Y$) are considered.

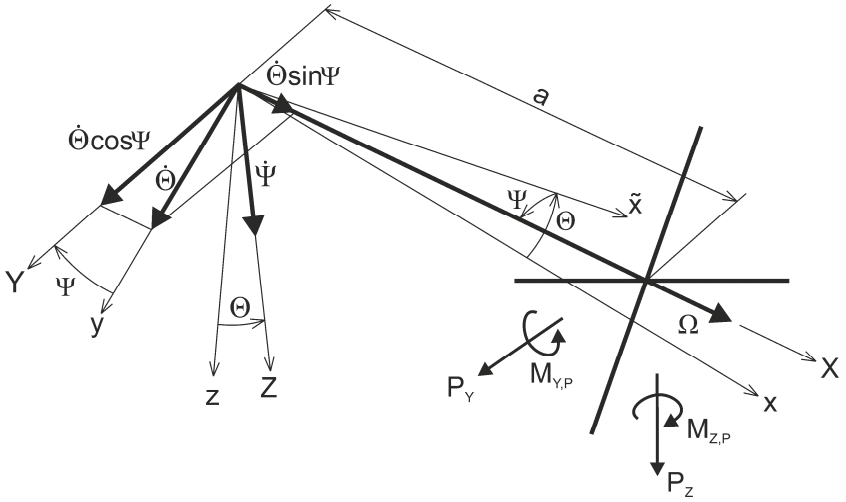

Figure 3: Kinematical scheme of gyroscopic system

When small angles are considered, the equations of motion become

$$\begin{aligned} J_Y\ddot{\Theta} + \frac{K_\Theta \gamma_\Theta}{\omega}\dot{\Theta} + J_X\Omega\,\dot{\Psi} + K_\Theta\Theta &= M_{Y,P} - aP_Z \\ J_Z\ddot{\Psi} + \frac{K_\Psi \gamma_\Psi}{\omega}\dot{\Psi} - J_X\Omega\dot{\Theta} + K_\Psi\Psi &= M_{Z,P} + aP_Y \end{aligned} \tag{1}$$

where a is the distance between the propeller plane and the vibration mode node point. Quantities γ_Ψ and γ_Θ are structural damping ratios of an engine yaw and pitch vibration modes. Neglecting the aerodynamic inertia terms ($\dot{\Theta}^* \approx \dot{\Theta}$; $\dot{\Psi}^* \approx \dot{\Psi}$), the propeller aerodynamic forces and moments at the propeller plane (P_Y; P_Z; $M_{Y,P}$; $M_{Z,P}$) are calculated as

$$P_Y = \frac{1}{2}\pi\,\rho\,V_\infty^2 R^2\left(c_{y\Theta}\Theta^* + c_{y\Psi}\Psi^* + c_{yq}\frac{\dot{\Theta}^* R}{V_\infty}\right)$$

$$P_Z = \frac{1}{2}\pi\,\rho\,V_\infty^2 R^2\left(c_{z\Theta}\Theta^* + c_{z\Psi}\Psi^* + c_{zr}\frac{\dot{\Psi}^* R}{V_\infty}\right)$$

$$M_{Y,P} = \pi\,\rho\,V_\infty^2 R^3\left(c_{m\Psi}\Psi^* + c_{mq}\frac{\dot{\Theta}^* R}{V_\infty}\right)$$

$$M_{Z,P} = \pi\,\rho\,V_\infty^2 R^3\left(c_{n\Theta}\Theta^* + c_{nr}\frac{\dot{\Psi}^* R}{V_\infty}\right) \tag{2}$$

where ρ is the air density and R is the propeller radius. Aerodynamic derivatives (c-terms) are given by the propeller blade integrals. These integrals are usually calculated according to Houbolt and Reed [1] or according to Ribner [2] [3]. We use quasi-steady theory [4] and the effective angles (Θ^*, Ψ^*) then become

$$\Theta^* = \left(\Theta - \frac{a\dot{\Theta}}{V_\infty}\right) - \frac{w_1}{V_\infty}$$

$$\Psi^* = \left(\Psi - \frac{a\dot{\Psi}}{V_\infty}\right) - \frac{w_2}{V_\infty} \tag{3}$$

The effective angles are given as the effective static angles (terms in brackets). Optionally, the downwash (w_1/V_∞) and sidewash (w_2/V_∞) angles behind the propeller describing the interference between a propeller and nacelle may be added. The induced downwash and sidewash terms, which are dependent on the reduced frequency, can be obtained from the lift solution by partitioning the interference coefficients. The downwash effect influences the aerodynamic stiffness matrix; the influence on the aerodynamic damping matrix is neglected. These interference effects may be important, especially for the wing-mounted engine aircraft, as the effect is usually destabilizing.

Finally, seeking for the critical (flutter) state (assuming the harmonic motion) has a character of an eigenvalue problem. The final whirl flutter matrix equation can be expressed as

$$\left(-\omega^2[M] + j\omega\left([D] + [G] + 2\pi\rho\,V_\infty\,R^4[D^A]\right) + \left([K] + \pi\,\rho\,V_\infty^2 R^3[K^A]\right)\right)\left|\begin{matrix}\bar{\Theta}\\ \bar{\Psi}\end{matrix}\right| = \{0\} \tag{4}$$

where [M] is the mass matrix, [D] is the structural damping matrix, [K] is the structural stiffness matrix. [D^A] and [K^A] are the aerodynamic damping and aerodynamic stiffness matrices, respectively. These matrices include aerodynamic derivatives (c-terms) and geometry of the system (a, R). Finally, [G] is the gyroscopic matrix. The critical state emerges when the angular velocity ω is real. The critical state can be reached by increasing either V_∞ or Ω. Increasing the propeller advance ratio (V_∞ / (ΩR)) has a destabilizing effect. Another important parameter is the distance of the propeller plane from the node points of the engine vibration modes. Structural damping is a significant stabilization factor. By contrast, the influence of the propeller thrust is negligible. This small influence comes from the fact that

variance of the aerodynamic derivatives of the thrusting propeller and windmilling propeller can be high in the low speed region, but at high velocities (where whirl flutter is expected), the variance is less than 5% [5]. For the rigid propeller blades, the whirl flutter inherently appears at the backward gyroscopic mode. The most critical state is $\omega_\Theta = \omega_\Psi$ when the interaction between both independent motions is maximal and the trajectory of the gyroscopic motion is circular.

The described model that considers a rigid propeller is obviously applicable to conventional propellers, for which the propeller blade frequencies are much higher compared to the nacelle pitch and yaw frequencies. For the large multi-bladed propellers of heavy turboprop aircraft, the assumption of a rigid propeller appears to be too conservative and the blade flexibility must also be modelled. Comprehensive information regarding the whirl flutter phenomenon can be found in [6] [7].

3 STANDARD ANALYTICAL APPROACH

In the standard approach, the input data are parameters of a structure and the outputs of the analysis are whirl flutter characteristics, i.e., V-g-f diagrams, and flutter speed and frequency. The demonstrated solution is based on the strip aerodynamic theory [8] for the rigid propeller at the windmilling mode. For aircraft structure, the unsteady doublet-lattice method is used in combination with the wing–body interference aerodynamic theory [9]. Flutter stability analysis is performed using the p-k method [10]. The basic flutter equation is expressed as

$$\left[[M_{hh}]\lambda^2 + \left([B_{hh}] - \frac{1}{4}\rho\,\bar{c}\,V_\infty\frac{[Q_{hh}^{Im}]}{k}\right)\lambda + \left([K_{hh}] - \frac{1}{2}\rho\,V_\infty^2[Q_{hh}^{Re}]\right)\right]\{u_h\} = 0 \tag{5}$$

where $[M_{hh}]$, $[B_{hh}]$ and $[K_{hh}]$ are the modal mass, damping and stiffness matrices, respectively, which are functions of the Mach number (M) and the reduced frequency (k). Aerodynamic loads are included in the damping and stiffness matrices. $[Q_{hh}^{Re}]$ and $[Q_{hh}^{Im}]$ are the real and the imaginary parts of a complex aerodynamic matrix, which is also a function of parameters M and k. The parameter ρ is the air density, $\bar{c}$ is a reference length, and $\{u_h\}$ is a modal amplitude vector. The eigenvalue λ is given as

$$\lambda = \omega\,(\gamma \pm j) \tag{6}$$

and γ is a transient decay rate coefficient. The structural damping coefficient (g) is expressed as

$$g = 2.\gamma \tag{7}$$

In the case of the standard approach, the solution for the whirl flutter is performed for multiple velocities. The resulting quantities are V-g-f curves, i.e., the dependences of the damping and frequencies of the analysed modes on the flight velocity. The state with the zero damping represents the critical flutter state and the corresponding flight velocity is the critical flutter speed.

4 OPTIMISATION-BASED ANALYTICAL APPROACH

4.1 Theoretical Background

The optimisation-based approach [11] [12] employs gradient-based algorithms [13] – [17] to obtain the whirl flutter solution. In this case, the flutter speed is set as an input parameter (certification speed), and the results are critical values of structural parameters. This solution enables to obtain the stability margin for the specified certification speed using the calculated critical structural parameters. The analysed states are then compared with respect to the structural parameters and the relationship to the stability margin only. Such an approach can save large amount of time because the number of whirl flutter analyses required by the regulations is dramatically reduced.

Two types of design responses (eigenvalue and flutter) are employed. The eigenvalue equation is:

$$([\mathrm{K}] - \lambda_n[\mathrm{M}])\{\phi_n\} = 0 \tag{8}$$

where λ_n and ϕ_n are the n^{th} eigenvalue and eigenvector, respectively; [K] is the structural stiffness; and [M] is the structural mass matrix. The equation is differentiated with respect to the i^{th} design variable x_i:

$$([\mathrm{K}] - \lambda_n[\mathrm{M}])\frac{\partial\{\phi_n\}}{\partial x_i} + \left(\frac{\partial[\mathrm{K}]}{\partial x_i} - \lambda_n\frac{\partial[\mathrm{M}]}{\partial x_i}\right)\{\phi_n\} = \frac{\partial\lambda_n}{\partial x_i}[\mathrm{M}]\{\phi_n\} \tag{9}$$

If equation (9) is premultiplied by ϕ_n^T, the first term becomes zero and it can then be solved for the eigenvalue derivatives:

$$\frac{\partial\lambda_n}{\partial x_i} = \frac{\{\phi_n\}^T\left(\frac{\partial[\mathrm{K}]}{\partial x_i} - \lambda_n\frac{\partial[\mathrm{M}]}{\partial x_i}\right)\{\phi_n\}}{\{\phi_n\}^T[\mathrm{M}]\{\phi_n\}} \tag{10}$$

The solution method used for equation (10) is based on the semi-analytical approach in practice. The derivatives of the mass and stiffness matrices are approximated using the finite differences. The equation is solved for each retained eigenvalue referenced in the design model and for each design variable.

The aeroelastic flutter stability matrix equation is given by equation (5), which represents the p-k method of the flutter solution. This is the only method applicable for the purpose of the design optimisation.

Flutter design response computes the rates of change of the transient decay rate coefficient γ with respect to changes of the design variables. This equation is differentiated with respect to the design variables ($\partial\gamma/\partial x_i$). The solution is semi-analytical in nature, with derivatives approximated using either forward differences or central differences.

Contrary to the standard solution, the optimisation-based whirl flutter solution is performed for a single velocity. The resulting quantities are structural parameters, for which the flutter speed is equal to the specified certification speed.

4.2 Solution for Half-span Model

Provided the half-span model is used for whirl flutter analysis, two design variables are defined: 1) effective stiffness of the engine attachment in pitch (K_Θ), and 2) effective stiffness of the engine attachment in yaw (K_Ψ). First, the preparatory step is performed. Either K_Θ or K_Ψ is selected as the design variable and the objective function (OBJ) is defined as the squared error of the yaw-to-pitch frequency ratio (f_Ψ/f_Θ) with respect to the selected target value $(f_\Psi/f_\Theta)_T$.

$$\mathrm{OBJ} = \left(\frac{f_\Psi}{f_\Theta} - \left(\frac{f_\Psi}{f_\Theta}\right)_T\right)^2 \tag{11}$$

Note that the yaw frequency is expected higher than the pitch frequency as is usual; however, the solution may be obtained regardless the frequency order. The resulting values of K_Θ and K_Ψ are the input values for the main optimisation. For the main optimisation, both K_Θ and K_Ψ are used as the design variables. The design constraints include the requirement to maintain the target frequency ratio, for which the ±2% band is usually used in the practical applications.

$$\left(\frac{\left(\frac{f_\Psi}{f_\Theta} - \left(\frac{f_\Psi}{f_\Theta}\right)_T\right)}{\frac{f_\Psi}{f_\Theta}}\right)^2 < 4.0e^{-4} \tag{12}$$

Another constraint requires the flutter stability (i.e., negative damping) at the selected certification speed (V_{CERT}).

$$g(V_{CERT}) < 0 \tag{13}$$

In the practical solution, the interval shift from the null value is given due to the numerical character of the solution, to prevent division by zero. The constraint is modified to

$$-\infty < \left(\frac{g(V_{CERT}) - 0.03}{0.1}\right) < -0.3 \tag{14}$$

The flutter constraint should also prevent another type of flutter instability below the certification speed that may be caused by the changes in the design variables. Typically, the modes within the frequency up to 100 - 120 Hz are included. The constraint should therefore be applied to all modes included in the solution.

The objective function is defined simply as the sum of the pitch and yaw frequencies.

$$\mathrm{OBJ} = (f_\Theta + f_\Psi) \tag{15}$$

As the output, we will obtain the engine pitch and yaw stiffnesses (K_Θ and K_Ψ), for which the flutter speed is equal to the specified certification speed (V_{CERT}) and the yaw-to-pitch frequency ratio (f_Ψ/f_Θ) is equal to the specified target value $(f_\Psi/f_\Theta)_T$. The described procedure is then repeated for several yaw-to-pitch frequency ratios, typically ranging from 1.05 to 2.0, to obtain enough points to construct a stability margin curve.

The procedure is applicable regardless of whether the downwash effect (see section 2) is included or not. If the downwash effects are to be included, the appropriate downwash terms must be calculated prior to the optimisation.

After any optimisation iteration, the cross-orthogonality correlation analysis of modes before and after the iteration is performed due to the possible switching of the mode order. If such a switch occurs, the modes must be re-ordered. The correlation analysis is performed using the Modal Assurance Criterion (MAC), which is expressed as

$$\mathrm{MAC}(\psi_1, \psi_2) = \frac{\left|\{\psi_1\}^t\{\psi_2\}\right|^2}{\left(\{\psi_1\}^t\{\psi_1\}\right)\left(\{\psi_2\}^t\{\psi_2\}\right)} \tag{16}$$

where ψ_1 and ψ_2 are the correlated mode shapes. Note that only the engine pitch and yaw modes must be correlated with the residual modes during the verification.

4.3 Solution for Full-span Model

Provided the full-span model is used, the solution includes four design variables: 1) effective stiffness of the engine attachment for symmetric pitch ($K_{S\Theta}$); 2) effective stiffness of the engine attachment for antisymmetric pitch ($K_{A\Theta}$); 3) effective stiffness of the engine attachment for symmetric yaw ($K_{S\Psi}$); and 4) effective stiffness of the engine attachment for antisymmetric yaw ($K_{A\Psi}$).

In the following description, we assume the typical frequency order by frequency, i.e., symmetric pitch, antisymmetric pitch, symmetric yaw and antisymmetric yaw.

The character of the whirl flutter instability is dependent on the relation between the directions of rotation of the two propellers. For the case of identical directions of propeller revolution (CW-CW or CCW-CCW), which is applied to the most of the practical applications, two mechanisms of the whirl flutter appear: 1) a combination of symmetric pitch and antisymmetric yaw modes (SΘ/AΨ) and 2) a combination of antisymmetric pitch and symmetric yaw modes (AΘ/SΨ). The former mechanism is more critical, i.e., the required pitch and yaw stiffness is higher. Therefore, it is sufficient to include just this mechanism into the certification analysis.

In cases with the inverse directions (i.e., CW-CCW or CCW-CW), whirl flutter is caused by either antisymmetric pitch and antisymmetric yaw or by symmetric pitch and symmetric yaw. We will expect the former case in the following text. Also note that CW denotes the clockwise direction and CCW denotes the counter-clockwise direction.

First, target ratios of pitch frequencies $(f_{A\Theta}/f_{S\Theta})_T$ and of yaw frequencies $(f_{A\Psi}/f_{S\Psi})_T$ are set according to the ground vibration test results or are guessed (by experience). The typical ratios for real aircraft structures range from 1.12 to 1.18.

The analogy of the target yaw-to-pitch ratio described in the previous section is the ratio of the critical flutter modes here, i.e., $(f_{A\Psi}/f_{S\Theta})_T$ for the identical directions of propeller revolution and $(f_{A\Psi}/f_{A\Theta})_T$ for the inverse directions of propeller revolution.

Similarly to the half-span model, the solution starts with the preparatory step to set the initial design variables for the main optimisation. The design constraint includes the requirement to maintain the highest frequency within the engine modes (typically antisymmetric yaw).

$$\left(\frac{f_{A\Psi} - f_{A\Psi T}}{f_{A\Psi T}}\right)^2 < 4.0e^{-4} \tag{17}$$

The objective function is defined as the frequency ratio error expressed as one of the following equations

$$OBJ = SSQ\left\{\left[\frac{f_{A\Theta}}{f_{S\Theta}} - \left(\frac{f_{A\Theta}}{f_{S\Theta}}\right)_T\right], \left[\frac{f_{A\Psi}}{f_{S\Psi}} - \left(\frac{f_{A\Psi}}{f_{S\Psi}}\right)_T\right], \left[\frac{f_{A\Psi}}{f_{S\Theta}} - \left(\frac{f_{A\Psi}}{f_{S\Theta}}\right)_T\right]\right\} \tag{18}$$

$$OBJ = SSQ\left\{\left[\frac{f_{A\Theta}}{f_{S\Theta}} - \left(\frac{f_{A\Theta}}{f_{S\Theta}}\right)_T\right], \left[\frac{f_{A\Psi}}{f_{S\Psi}} - \left(\frac{f_{A\Psi}}{f_{S\Psi}}\right)_T\right], \left[\frac{f_{A\Psi}}{f_{A\Theta}} - \left(\frac{f_{A\Psi}}{f_{A\Theta}}\right)_T\right]\right\} \tag{19}$$

where SSQ denotes for the sum of squares. Equation (18) is applicable to the case of identical directions of propeller rotation, while equation (19) is applicable to the case of inverse directions of propeller rotation.

The main optimisation is performed similarly to that for the half-span model. The design constraints again include the requirements to maintain the frequency ratios, within the ±2% band

$$\left(\frac{\left(\frac{f_{A\Theta}}{f_{S\Theta}} - \left(\frac{f_{A\Theta}}{f_{S\Theta}}\right)_T\right)}{\frac{f_{A\Theta}}{f_{S\Theta}}}\right)^2 < 4.0e^{-4} \tag{20}$$

$$\left(\frac{\left(\frac{f_{A\Psi}}{f_{S\Psi}} - \left(\frac{f_{A\Psi}}{f_{S\Psi}}\right)_T\right)}{\frac{f_{A\Psi}}{f_{S\Psi}}}\right)^2 < 4.0e^{-4} \tag{21}$$

and

$$\left(\frac{\left(\frac{f_{A\Psi}}{f_{S\Theta}} - \left(\frac{f_{A\Psi}}{f_{S\Theta}}\right)_T\right)}{\frac{f_{A\Psi}}{f_{S\Theta}}}\right)^2 < 4.0e^{-4} \tag{22}$$

or

$$\left(\frac{\left(\frac{f_{A\Psi}}{f_{A\Theta}} - \left(\frac{f_{A\Psi}}{f_{A\Theta}} \right)_T \right)}{\frac{f_{A\Psi}}{f_{A\Theta}}} \right)^2 < 4.0e^{-4} \tag{23}$$

Again, equation (22) is applicable to the case of identical directions of propeller rotation, while equation (23) is applicable to the case of inverse directions of propeller rotation. The constraint on flutter stability (i.e., negative damping) at the selected certification speed V_{CERT} is expressed in the same way as for the half-span model, i.e., by equation (14). The objective function is also defined similarly to that for the half-span model, i.e., as the frequency sum, expressed here as

$$OBJ = SUM(f_{S\Theta}, f_{A\Theta}, f_{S\Psi}, f_{A\Psi}) \tag{24}$$

Similarly to the half-span model, the described procedure is then repeated for several critical flutter mode ratios, typically ranging from 1.05 to 2.0, to obtain enough points to construct a stability margin curve. The notes regarding the downwash effect and the mode switches mentioned in section 4.2 are also valid for the full-span model.

5 CERTIFICATION ACCORDING FAR/CS 23 STANDARD

FAR / CS 23 represent the simpler category of standards, applicable to the smaller turboprop aircraft. The whirl flutter-related requirement included in §629(e) is applicable for all configurations of aircraft regardless the number and placement of engine(s). §629(e)(1) includes the main requirement to evidence the stability within the required V-H envelope, while §629(e)(2) requires the variation of structural parameters such as the stiffness and damping of the power plant attachment. The latter represents the influence of the variance of the power plant mount structural parameters when simulating the possible changes due to structural damage (e.g., deterioration of engine mount isolators).

In the following text, we will consider standard twin wing-mounted tractor-engine aircraft configuration. In terms of mass configurations, whirl flutter analysis must include all wing mass configurations, especially fuel load variation. Contrary to that the payload does not have a significant influence. Analyses are performed just for the certification altitude, which is the most critical with respect to both whirl flutter and the value of certification speed ($1.2*V_{DTAS}$). In the application example, the certification altitude is H_{CERT} = 4267 m (14 000 ft).

Inertia characteristics of rotating parts must be considered with respect to the directions of rotation of a particular part (generator, turbine, propeller), revolutions are usually normalised to a propeller revolutions. For the purpose of certification analysis, the most critical mode of the propeller and engine revolutions should be considered, i.e. the mode that produce the maximal normalised moment of inertia of the rotating parts.

To comply with the main requirement (§629(e)(1)), the nominal state analyses are performed. For this purpose, the standard approach is employed. Analyses are performed sequentially (configuration-by-configuration). The resulting flutter speed is compared to the certification velocity according to the flight envelope. Figure 4 shows an example of a V-g-f diagram of

such a calculation for a single mass configuration. No flutter instability is indicated up to the certification velocity, which is 191.4 m/s in this case, and therefore, the regulation requirement is fulfilled.

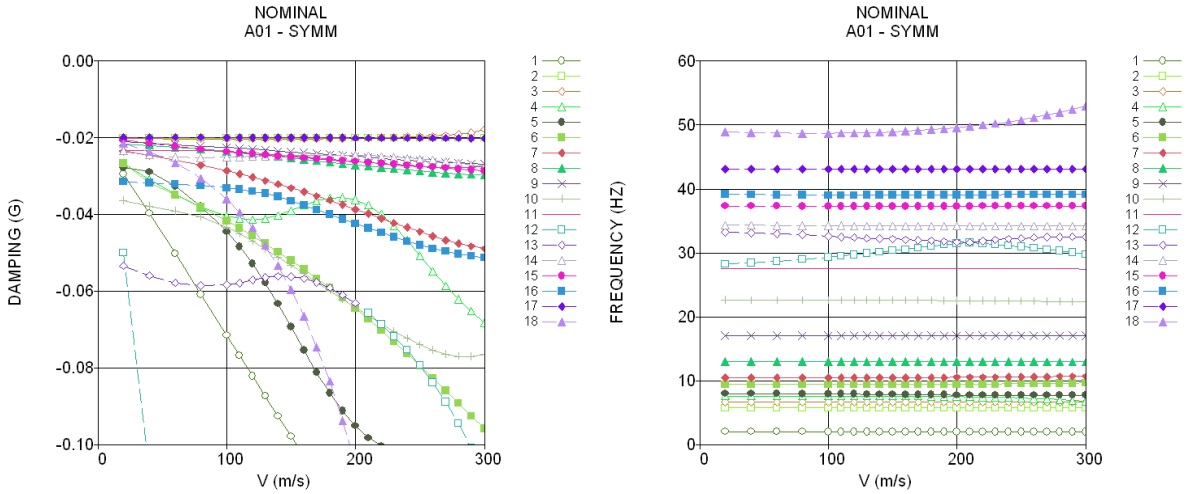

(a) (b)

Figure 4: Whirl flutter calculation (V-g-f) diagram, (a) damping, (b) frequency, nominal state

To comply with the parameter variation requirement (§629(e)(2)), parametric studies that may include huge numbers of analyses would be necessary and such an approach would become ineffective. Therefore, the analysis of stability margins using optimisation-based approach is good for this purpose. In this approach, the flutter speed is set equal to the certification speed, and the results are margin values of structural parameters. The stability margin then can be obtained and the relationship of parameters (e.g. engine attachment stiffness, engine pitch and yaw frequency) with respect to the margin may be evaluated. Such an approach can save large amount of time because the number of required analyses is dramatically reduced. Figure 5 shows an example of a V-g-f diagram of optimisation-based calculation in which flutter speed is equal to the certification velocity (191.4 m/s). Flutter mode (#2) is the engine pitch vibration mode.

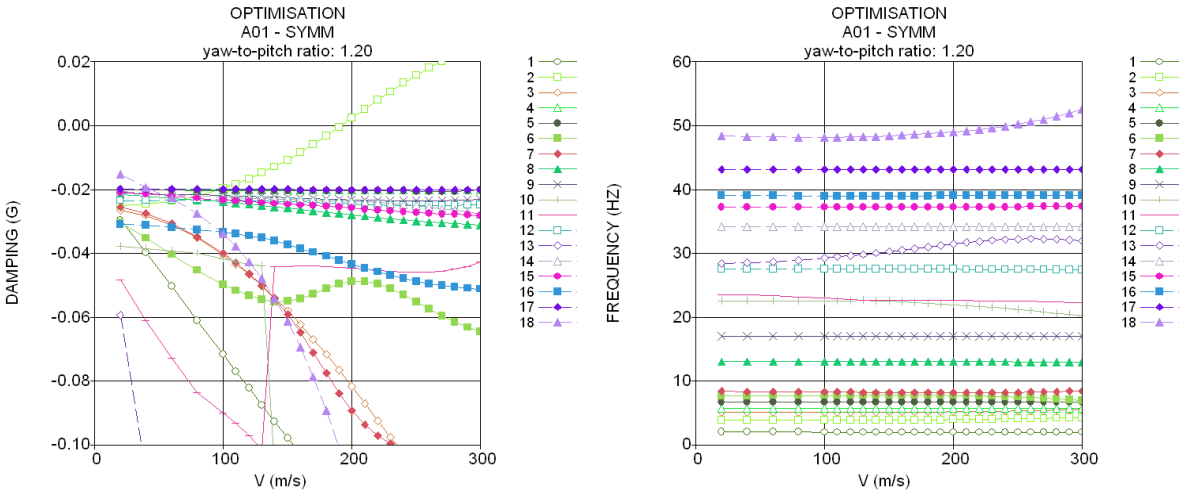

(a) (b)

Figure 5: Whirl flutter calculation (V-g-f) diagram, (a) damping, (b) frequency, optimisation-based calculation

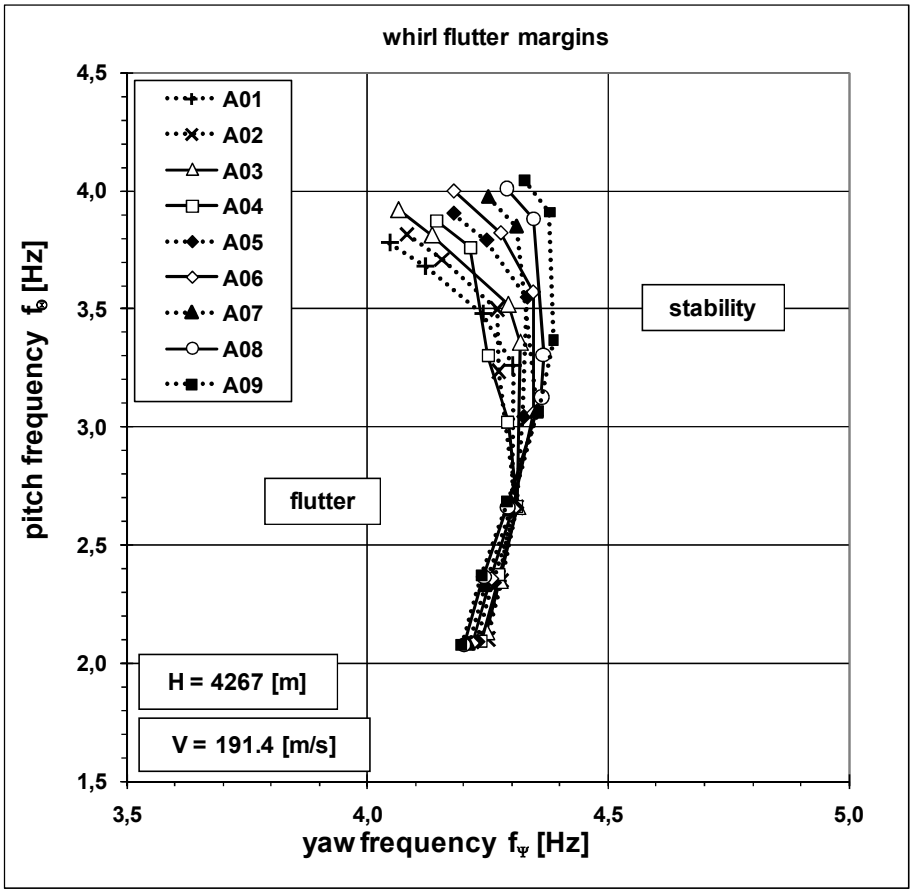

Figure 6: Whirl flutter stability margins for multiple mass configurations

Calculations are performed for several values of the yaw-to-pitch frequency ratio to construct a stability margin curve. Stability margins are then constructed for all applicable mass configurations, as shown in figure 6.

Stability margins may be constructed either with respect to engine yaw and pitch attachment effective stiffness or with respect to the engine yaw and pitch vibration frequency. The frequency-based margin may be then compared with the engine vibration frequencies, obtained by the GVT or analytically, to evaluate the rate of reserve as shown in figure 7. The dashed line represents the (+/-) 30% variance margin in engine attachment stiffness. Another parameter to be evaluated is the damping. This is provided using the calculation with very low structural damping, represented by the damping of $g = 0.005$, while the standard structural damping included in the analyses is $g = 0.02$. As obvious from figure 7, there is sufficient reserve in stability of the nominal state (including parameter variations) with respect to the stability margin, and therefore, the regulation requirements are fulfilled.

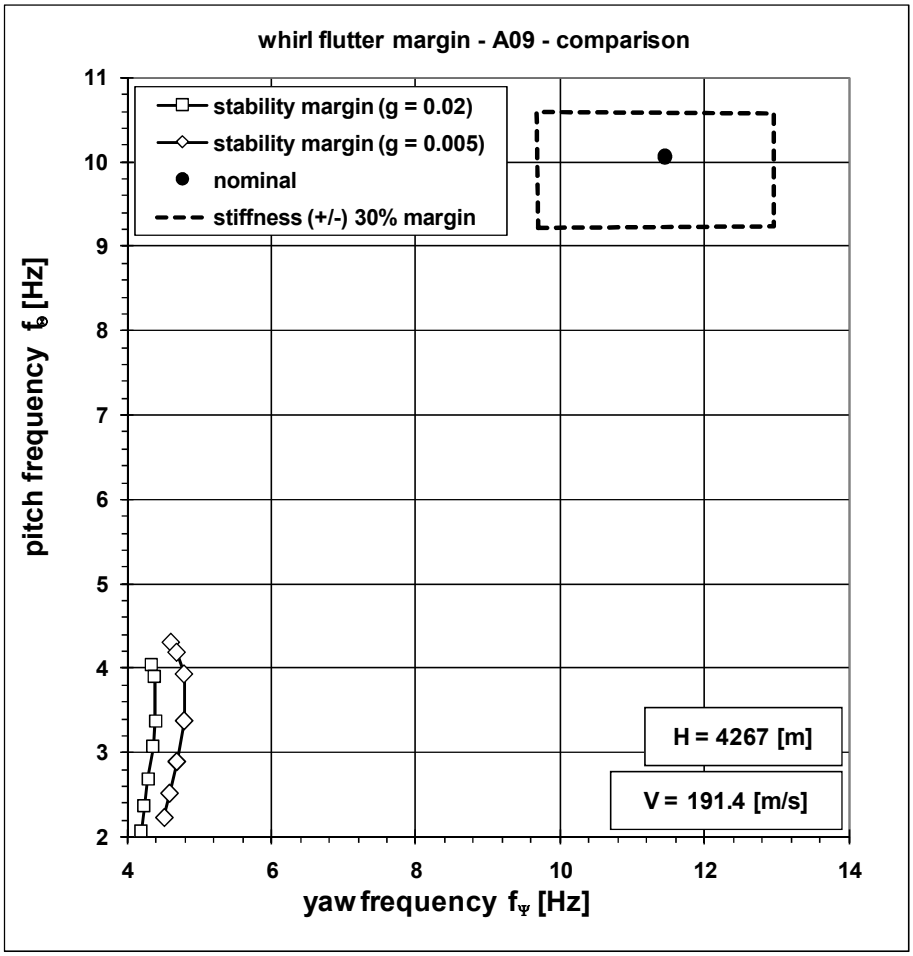

Figure 7: Whirl flutter stability margin evaluation

6 CERTIFICATION ACCORDING FAR/CS 25 STANDARD

FAR / CS 25 represent the standard category applicable to larger turboprops. As in the previous section, we will consider standard twin wing-mounted tractor-engine aircraft configuration. In addition to the requirements, which are similar to those of the previous case, some specific states of failure, malfunctions and adverse conditions are required to be analysed as well. These states are:

1) Critical fuel load conditions. This requirement includes the analysis of unsymmetrical conditions of the fuel loading that may come from the mismanagement of the fuel. In this case, fuel model is modified while the power plants model shows the nominal conditions.

2) Failure of any single element supporting any engine. This requirement includes in particular the failure of any single engine bed truss. The failure conditions are introduced into a single power plant mount system while other power plant mount systems use a nominal condition. All engines show the nominal condition.

3) Failure of any single element of the engine. This requirement includes, in particular, the failure of any single engine mount-isolator. The failure conditions are introduced into a single power plant mount system while other ones show nominal conditions. All engine mounts were used under nominal conditions.

4) Absence of aerodynamic and gyroscopic forces due to feathered propellers. The failure states defined in this section represent the states of a nonrotating engine and a nonrotating feathered propeller. The power plant system under such conditions generates no aerodynamic or gyroscopic forces. In addition, the single feathered propeller or rotating device failure must be coupled with the failures of the engine mount and the engine.

5) Any single propeller overspeed. The power plant system under such conditions generates maximal aerodynamic and gyroscopic forces. The condition of overspeed must include the highest likely overspeed of both engine and propeller. The state of overspeed is applied to any single propeller while the other ones are under the nominal conditions.

6) Other failure states. It includes failure states coming from the damage-tolerance analysis, from bird strike damages and from damages of the control systems, the stability augmentation systems and other equipment systems and installations.

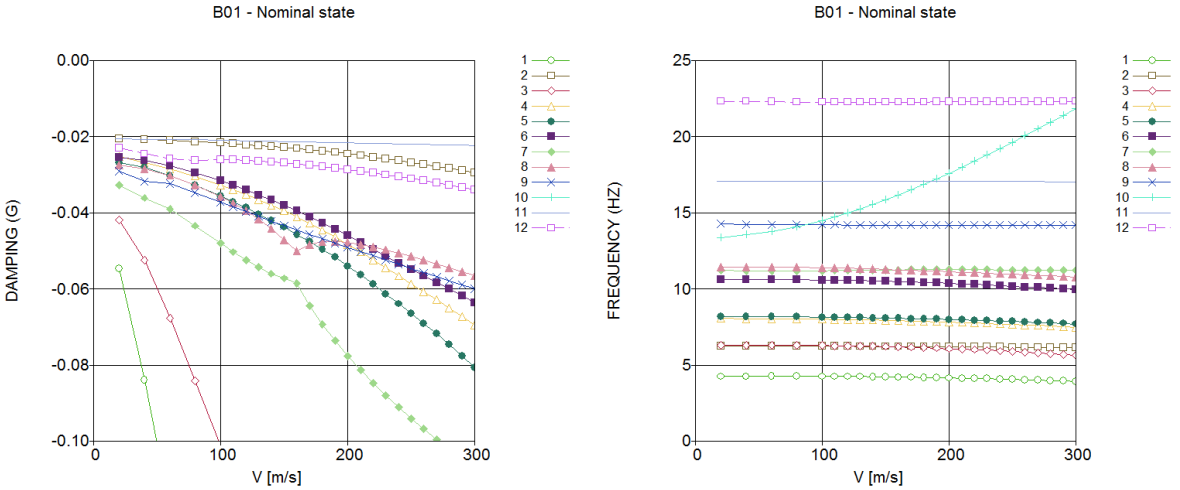

Figure 8: V-g-f diagram, nominal state, $f_{S\Theta}$ = 8.16 Hz, $f_{A\Theta}$ = 8.32 Hz, $f_{S\Psi}$ = 10.50 Hz, $f_{A\Theta}$ = 11.31 Hz

All mentioned requirements lead to the specific unsymmetrical conditions; therefore, only full-span model is applicable. For the purpose of certification, analyses may be performed sequentially, state-by-state, using standard approach. Figure 8 and 9 show the comparison of a nominal state analysis and a failure state, represented by the starboard engine attachment stiffness reduction by 30%. However, as obvious from the figures, the standard approach gives no information regarding the influence of a particular failure state on the whirl flutter stability, compare to the nominal conditions. Provided such information is required from any reason, the optimisation-based approach may be employed and the stability margins, representing the specific failure states, may be constructed and compared with the appropriate nominal state. The examples are shown in figures 10 and 11. Figure 10 shows the failure state of a single (starboard) feathered propeller. Compare to the nominal state, the required yaw and pitch frequency to ensure the stability at the certification speed is lower, thus, the effect on the whirl flutter stability is positive. Figure 11 shows the failure states of a single propeller under- and overspeed. The figure includes the nominal state and the states of a single (starboard) propeller with reduced and with increased revolutions (by 15%). Compare to the nominal state, reduced revolutions make the system more stable while the increased revolutions have destabilising effect.

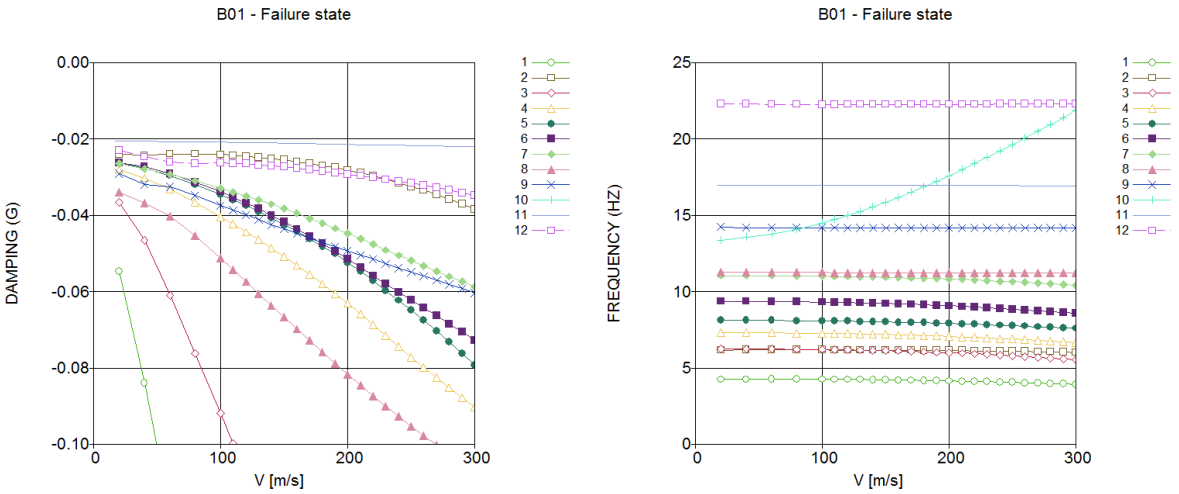

Figure 9: V-g-f diagram, failure state, reduction of starboard engine attachment stiffness, $f_{\Theta R}$ = 7.45 Hz, $f_{\Theta L}$ = 8.25 Hz, $f_{\Psi R}$ = 9.19 Hz, $f_{\Theta L}$ = 10.98 Hz

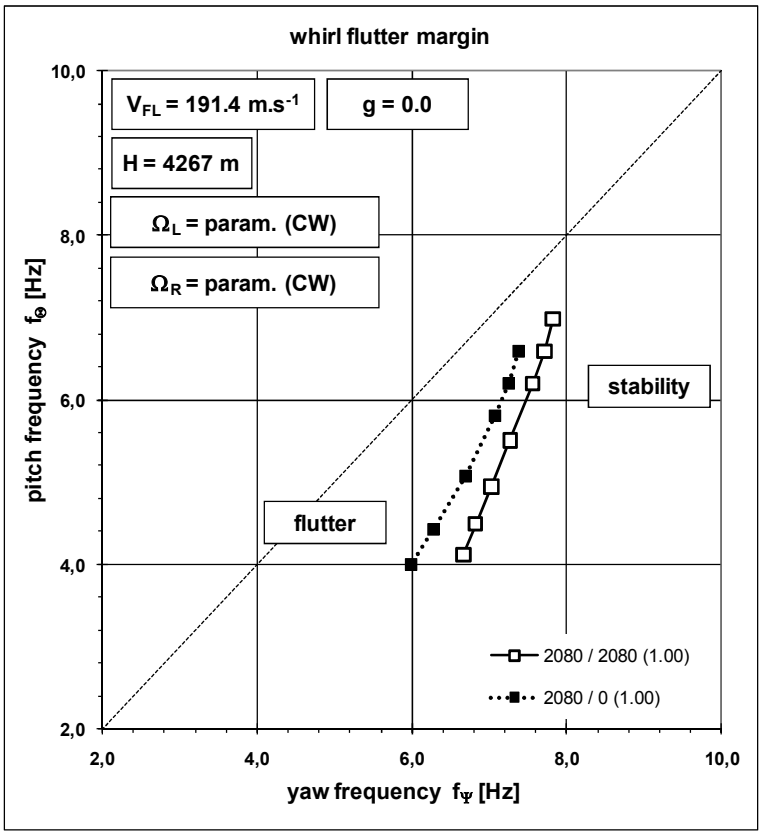

Figure 10: Stability margins, comparison of a symmetric case (2080 rpm) and a case of a single feathered propeller (2080 / 0 rpm)

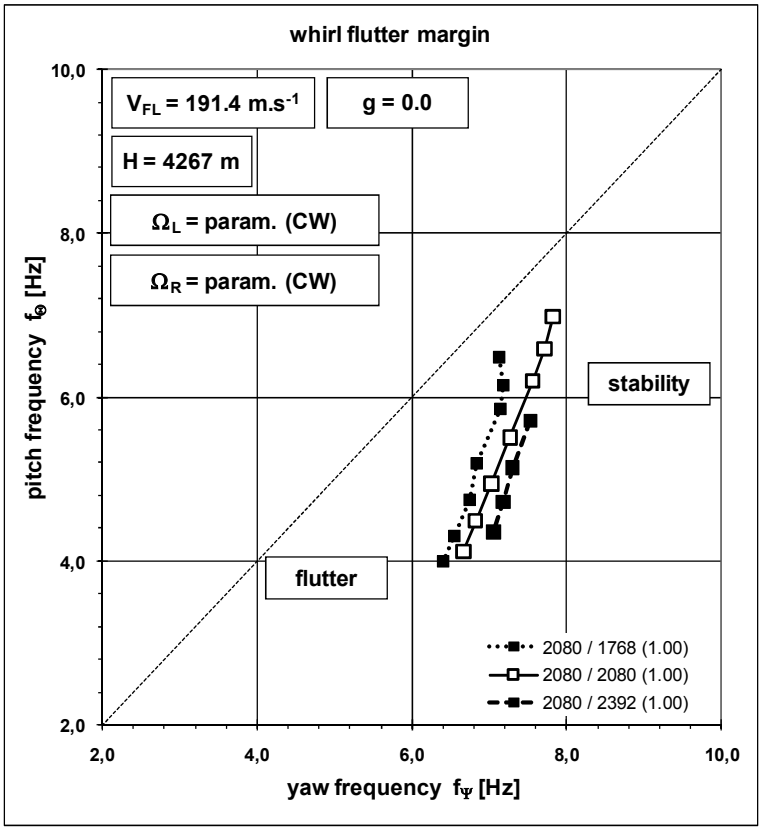

Figure 11: Stability margins, comparison of a symmetric case (2080 rpm) and cases of unsymmetric revolutions: a single propeller reduced rpm (2080 / 1768) and a single propeller increased rpm (2080 / 2392)

7 CONCLUSION

This paper presented the methodologies of compliance with whirl flutter-related requirements of FAR / CS 23 and 25 regulation standards. Methodologies are demonstrated on the example of a twin wing-mounted engine aircraft. Two approaches to the analysis are described: 1) Standard approach used to comply with the main requirement of the FAR / CS 23 standard (§629(e)(1)) and 2) Optimisation-based approach used to comply with the requirement of parameter variations of the FAR / CS 23 standard §629(e)(2). For compliance with FAR / CS 25 standard, the additional requirements to analyse specific failure states and adverse condition states are described.

REFERENCES

[1] Houbolt, J. C. and Reed, W. H. (1962) Propeller – Nacelle Whirl Flutter. *Journal of the Aerospace Sciences,* 29(3), 333-346.

[2] Ribner, H. S. (1945) Propellers in Yaw. Report 820, NACA.

[3] Ribner, H. S. (1945) Formulas for Propellers in Yaw and charts of the Side – Force Derivatives. Report 819, NACA.

[4] Forsching, H. W. (1974) *Grundlagen der Aeroelastik*, Springer – Verlag.

[5] Reed, W. H. and Bennett, R. M. (1963) Propeller Whirl Flutter Considerations for V/STOL Aircraft. *CAL/TRECOM Symposium*, Buffalo, NY, USA.

[6] Čečrdle, J. (2015) *Whirl Flutter of Turboprop Aircraft Structures*. Oxford: Elsevier Science.

[7] Čečrdle, J. (2018). Aeroelastic Stability of Turboprop Aircraft: Whirl Flutter. In: *Flight Physics – Models, Techniques and Technologies*, Konstantin Volkov (Ed.), 139-158. InTech Publications. Rijeka.

[8] Theodorsen, T. (1935) General Theory of Aerodynamic Instability and the Mechanism of Flutter, Report 496, NACA.

[9] Giessing, J. P., Kalman, T. P. and Rodden, W. P. (1972) Subsonic Steady and Oscillatory Aerodynamics for Multiple Interfering Wings and Bodies. *Journal of Aircraft*, 9, 693-702.

[10] Rodden, W. P. and Bellinger, E. D. (1982) Aerodynamic Lag Functions, Divergence, and the British Flutter Method. *Journal of Aircraft,* 19, 596-598.

[11] Čečrdle, J. (2017). Whirl Flutter Optimisation-based Solution of Twin Turboprop Aircraft Using a Full-span Model. *Applied and Computational Mechanics*, 11(1), 5–22.

[12] Čečrdle, J. (2012). Analysis of Twin Turboprop Aircraft Whirl-Flutter Stability Boundaries. *Journal of Aircraft*, 49(6), 1718–1725.

[13] Johnson, E.H. and Reymond, M.A. (1991) Multidisciplinary Aeroelastic Analysis and Design Using MSC/NASTRAN, In: *AIAA/ASME/ASCE/AHS/ASG 32nd Structures, Structural Dynamics and Materials Conference.* Baltimore, MD, USA.

[14] Climent, H. and Johnson, E.H. (1993) Aeroelastic Optimization Using MSC/NASTRAN. In: *International Forum on Aeroelasticity and Structural Dynamics*, Strasbourg, France

[15] Lewis, A.P. (1991) A NASTRAN DMAP Procedure for Aeroelastic Design Sensitivity Analysis, In: *18th MSC European Users' Conference*.

[16] Lahey, R.S. (1983) Design Sensitivity Analysis Using MSC/NASTRAN, In: *MSC World Users Conference*.

[17] Heinze, P., Schierenbeck, D. and Niemann, L. (1989) Structural Optimization in View of Aeroelastic Constraints Based on MSC/NASTRAN FE Calculations. In: *16th MSC European Users' Conference*.

COPYRIGHT STATEMENT